Nuclear Instruments and Methods in Physics Research A 621 (2010) 620–626

Contents lists available at ScienceDirect

Nuclear Instruments and Methods in Physics Research A

journal homepage: www.elsevier.com/locate/nima

Simulation of heat transfer in zone plate optics irradiated by X-ray free electron laser radiation

D. Nilsson [a,*], A. Holmberg [a], H. Sinn [b], U. Vogt [a]

[a] Biomedical and X-ray Physics, Royal Institute of Technology, KTH-AlbaNova, SE-106 91 Stockholm, Sweden
[b] European XFEL – Notkestrasse 85, D-22607 Hamburg, Germany

ARTICLE INFO

Article history:
Received 8 February 2010
Received in revised form
5 March 2010
Accepted 12 March 2010
Available online 18 March 2010

Keywords:
X-ray optics
Zone plate
XFEL
Heat transfer

ABSTRACT

Zone plates are high quality optics that have the potential to provide diffraction-limited nano-focusing of hard X-ray free electron laser radiation. The present publication investigates theoretically the temperature behavior of metal zone plates on a diamond substrate irradiated by 0.1 nm X-rays from the European X-ray Free Electron Laser. The heat transfer in the optic is simulated by solving the transient heat equation with the finite element method. Two different zone plate designs are considered, one small zone plate placed in the direct beam and one larger zone plate after the monochromator. The main result is that for all investigated cases the maximum temperature in the metal zone plate layer is at least a factor 2 below the melting point of the respective material, proving the efficiency of the proposed cooling scheme. However, zone plates in the direct beam experience large and rapid temperature fluctuations of several hundred Kelvin that might prove fatal to the optic. The situation is different for optics behind the monochromator with fluctuations in the 20 K range and maximum temperatures well below room temperature. The simulation results give valuable indications on the temperature behavior to be expected and are a basis for future experimental heat transfer and mechanical stability investigations of fabricated nanostructures.

© 2010 Elsevier B.V. All rights reserved.

1. Introduction

Free electron lasers (FELs) emitting in the hard X-ray regime around 0.1 nm wavelength are upcoming large scale facilities at few places worldwide. While the Linac Coherent Light Source (LCLS) [1] in the USA already started its operation, the European X-ray Free Electron Laser (XFEL) in Germany [2] and the Spring-8 Compact SASE Source (SCSS) in Japan [3] are under development. It is envisaged that these machines will enable new research possibilities in many fields, from basic science to medicine. One of the major challenges is how to focus the hard X-ray laser beam with a typical diameter in the mm range down to spot sizes in the range of 100 nm or less as required by many application experiments. One possibility is the use of diffractive zone plate optics, i.e., circular gratings with decreasing grating constant. In the present article, we propose a zone plate design that should survive a single FEL pulse and investigate with the help of transient heat transfer simulations if zone plates can withstand the high average heat load created by the partial absorption of the FEL X-ray beam in the zone plate material.

In general, several possibilities based on reflective, refractive or diffractive optical devices exist in order to focus an X-ray beam. The method of choice will often depend on the focal spot size required for a specific experiment. For focus diameters below 100 nm and a hard X-ray free electron laser beam, three different possibilities are under consideration, namely double-mirror Kirkpatrick-Baez systems [4], compound refractive lenses [5] or diffractive zone plates. While every system has its advantages and disadvantages, zone plates are of special interest since they are the X-ray optics that presently show the highest special resolution approaching the 10 nm regime [6–8]. At the same time, they are diffraction-limited which means that they do not introduce aberrations into the wavefront behind the zone plate. This might be very important for certain types of experiments. The most prominent example is single molecule diffraction imaging which tries to reconstruct the structure of, e.g., a protein from its diffraction pattern by iterative algorithms [9]. A third advantage of zone plates is the fact that they are single elements that are easily and quickly aligned to the X-ray beam, an aspect of great practical importance since beamtime at X-ray FELs is very limited.

Despite the obvious benefits of zone plate optics the major question presently unknown is for how long a zone plate can withstand the high-intensity FEL beam. This question has been under discussion for some time now and experimental experience

* Corresponding author at: KTH-BioX, Albanova University Center, SE-106 91 Stockholm, Sweden. Tel.: +46 8 5537 8038; fax: +46 8 5537 8466.
E-mail address: daniel.nilsson@biox.kth.se (D. Nilsson).

0168-9002/$ - see front matter © 2010 Elsevier B.V. All rights reserved.
doi:10.1016/j.nima.2010.03.115

is limited to zone plates placed in a direct, unfocused extreme-ultraviolet FEL beam [10]. Moreover, the technical design report (TDR) of the European XFEL writes that "the lifetime of zone plates may turn as short as a single pulse" [2]. Even in this case a zone plate can still be useful since the focusing of the light might take place before the optic explodes. Consequently, zone plates lasting only a single shot have already been tested as focusing optics in a diffraction experiment at the FLASH soft X-ray free electron laser in Hamburg. However, the high costs and inefficient use of beam time of this method are serious limitations.

In the present publication we propose the design of a zone plate that should survive a single X-ray FEL pulse and that is based on materials that are compatible with current nanofabrication methods for zone plates. The major challenge then is if the zone plate can handle the long-term average heat load induced by the fractional absorption of the X-rays in the zone plate material. This is especially true for the European XFEL with its special time structure consisting of pulse trains rather than isolated single pulses [2]. We use the finite-element method [11] to calculate the transient heat transfer in the optic in order to investigate the temperature behavior at different places on the optic. This temperature should be well below the melting temperature of the used materials as a first necessary criterion for the survival of the optic. Although there are many other important issues that have to be investigated both theoretically and experimentally before a definite statement for the long-term usefulness of zone plates can be made, we limit the present study to heat transfer investigations since they already can give recommendations for the direction of further research. Moreover, we limit the calculation to the case of diffraction-limited focusing since we believe that this ability is the major advantage of a zone plate compared to other optics.

2. Zone plate design

2.1. X-ray free electron laser beam parameters

Table 1 summarizes the most basic parameters of the three facilities mentioned in the introduction. For the heat load on the zone plate the most important factors are the absorbed energy/volume per pulse and the repetition rate of the pulses. The amount of absorbed energy in one pulse is determined by the wavelength, the number of photons per pulse, the transverse size of the beam and the material used for the zone plate and substrate.

The number of photons per pulse is roughly 10^{12} for all three facilities and the wavelength is either 0.1 nm as in the case of XFEL and SCSS or 0.15 nm as in the case of LCLS. The largest difference between the three facilities is the pulse structure. LCLS and SCSS have evenly spaced pulses of repetition rate 120 and 60 Hz, respectively. The use of a superconducting linac at the XFEL enables a more complex time structure consisting of 10 bunch trains per second where each bunch train is 0.6 ms long and consists of 3000 pulses with 200 ns spacing. The amount of energy in one pulse is of the same order of magnitude for all three facilities but the pulse structure at XFEL will be considerably more demanding for the optics from a heat load perspective. For this reason, this paper will consider the heat load at the XFEL and uses the beam parameters of the SASE1 undulator in the simulations.

Table 1
Parameters of the three hard X-ray free electron laser facilities [1–3].

	XFEL SASE1	LCLS	SCSS
Wavelength	0.1 nm	0.15 nm	0.1 nm
Pulse duration	100 fs	80 fs	500 fs
Photons/pulse	1e12	1e12	7.6e11
Pulses/second	30000	120	60

2.2. Choice of zone plate parameters and materials

The first-order focal spot size δ of a zone plate illuminated by a plane wave is given by:

$$\delta = 1.22\Delta r \quad (1)$$

This makes the outermost zone width Δr the most important zone plate parameter. A zone plate focuses light into many diffraction orders and the efficiency of the first-order focus is determined by the thickness d and the optical properties of the grating material [12]. In general, for hard X-rays d will always be much larger than Δr, so the maximum possible thickness of a certain zone plate is limited by the ability to fabricate these high-aspect-ratio structures. State-of-the-art nanofabrication techniques can achieve zone plate aspect ratios up to 15:1 [13], but the exact value will strongly depend on the desired Δr. The smaller Δr, the smaller will be the possible aspect ratio and therefore also the zone plate efficiency. For the following simulations we chose $\Delta r = 100$ nm and $d = 1$ μm, i.e., an aspect ratio of 10:1 as a compromise that lies well within current nanofabrication capabilities.

The diameter D of a zone plate is given by Δr and the total number of zones N:

$$D = 4N\Delta r \quad (2)$$

If we consider diffraction-limited focusing, the number of zones N should not be larger than the inverse of the bandwidth $\Delta E/E$ [14]. For a zone plate with $\Delta r = 100$ nm and a bandwidth of $\Delta E/E = 10^{-3}$ this results in 1000 zones and a corresponding diameter of 400 μm. If this size is compared to the XFEL beam diameter of 982 μm full width half maximum (FWHM) in the experimental hall 980 m behind the SASE1 undulator it is clear that not all photons are collected by the zone plate. To solve this problem one can think of simply increasing the diameter of the zone plate but this also increases the number of zones and the focus is no longer diffraction-limited. In order to maintain the diffraction-limited focus, a possible solution is to use a monochromator that reduces the bandwidth to $\Delta E/E = 10^{-4}$. The lower bandwidth enables the use of a zone plate as large as 4 mm in diameter ($N = 10000$) which can collect the full beam. However, using a monochromator has the drawback of decreasing the number of photons in the beam to 10% of the original value. On the other hand, a larger zone plate area can partly compensate for this and from a heat load point-of-view the placement of the optic behind the monochromator is preferable. It is interesting to note that the final beam width of the XFEL SASE1 is still under discussion and might be adjustable, to both larger and smaller diameters, compared to the original value of 982 μm (FWHM) discussed in the TDR. Therefore, this paper investigates both a smaller zone plate without a monochromator and a larger zone plate with a monochromator.

In order to achieve high diffraction efficiency for a 1 μm thick zone plate at 0.1 nm wavelength the optic should ideally be made of a high-Z material. Zone plates for hard X-rays have been fabricated in materials such as gold [15], tantalum [16], iridium [17], and tungsten [18]. The first-order efficiencies as a function of grating thickness at $\lambda = 0.1$ nm are shown for some of these materials in Fig. 1. The efficiency does not vary much between the different materials and all are good candidates from an efficiency perspective. It should be noted that the efficiency is a result of both absorption and phase shift in the zone plate structures.

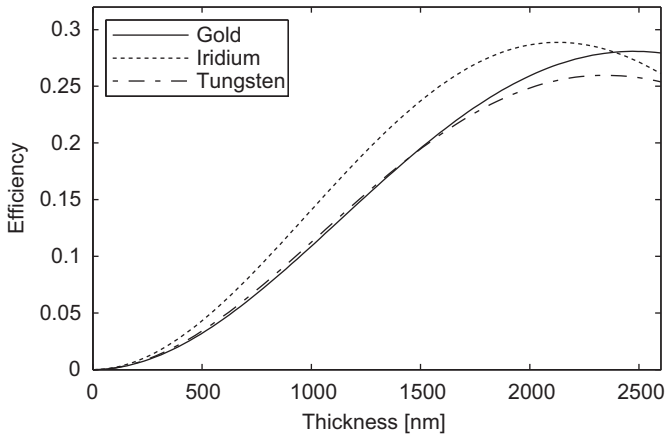

Fig. 1. First order diffraction efficiency for different zone plate material thicknesses at wavelength $\lambda=0.1$ nm.

However, the disadvantage of a zone plate made from a high-Z material is a high X-ray absorption in the material. For example, a 1 μm gold layer absorbs 27% at $\lambda=0.1$ nm so for a pulse energy of 2 mJ ($=10^{12}$ photons) the temperature increase in the layer will be significant. If the zone plate should have a chance to survive one pulse, the temperature directly after the pulse should be well below the melting temperature of the material. Moreover, the substrate has to transfer away enough heat before the next pulse arrives. Otherwise, the temperature will quickly build up and the zone plate might evaporate after a few pulses. The substrate material, geometry and the cooling scheme used determine the amount of heat transferred away between two pulses. The important material parameter is the thermal diffusivity α defined as $\alpha=k/\rho C_p$ where k is the thermal conductivity, ρ is the density and C_p is the specific heat capacity. At both room temperature and liquid nitrogen temperature, the substrate material with highest thermal diffusivity is diamond. Diamond also has the advantage of being a light element and as such has a low absorption of X-rays. The thickness of the substrate should be as thick as possible to have a large thermal bulk but at the same time thin enough to minimize absorption. Diamond is commercially available in chemical vapor deposition (CVD) form in many different thicknesses. Choosing a thickness of 100 μm is a good compromise, providing good thermal properties and absorbing only 4% at $\lambda=0.1$ nm. Cooling the substrate with liquid nitrogen (77 K) further increases the thermal performance since the thermal conductivity increases with decreasing temperature.

An alternative to a metal zone plate on a diamond substrate would be a zone plate made entirely out of a low-Z material like silicon [19] or diamond where the zone plate pattern is directly transferred into the substrate. The reduced absorption, as compared to a metal zone plate, greatly reduces heat generation in the zone plate structure. The problem is that extremely high aspect ratios are needed in order to achieve good diffraction efficiency. As an example, a thickness of 1 μm diamond would give an efficiency of merely 1%. However, if one were able to fabricate a 10 μm thick diamond structure it is possible to reach a maximum theoretical efficiency of 40%. Unfortunately, for a zone width of $\Delta r=100$ nm this is far beyond today's nanofabrication possibilities.

To sum up, this paper investigates two possible designs. Both consist of a 1 μm thick zone plate made of gold, iridium or tungsten. These materials were chosen because they represent a large span of important thermal properties (see Table 2) as described in the next section. The optics are fabricated on 100 μm thick CVD diamond substrates. The differences between the two designs are the number of zones and the diameter. If the zone plate is to be placed in the direct beam an optic with 1000 zones and a diameter of 400 μm is considered. When using a monochromator the diameter is chosen to be 2 mm, corresponding to 5000 zones. Fig. 3 shows the geometry of the two zone plates including the substrate and cooling scheme. The substrate faces towards the XFEL beam absorbing 4% of the incoming radiation and thereby reducing the amount that hits the metal zone plate layers. To increase the efficiency of the cooling, the substrate is bonded to a diamond cone that is cooled at the edge [20]. A sketch of the diamond cone and zone plate is shown in Fig. 2. No limiting aperture is assumed in front of the zone plate so also the cone part is exposed to the XFEL beam. For the larger 2 mm zone plate, no cone is needed and it is possible to apply the cooling directly to the edge of the substrate.

Table 2
Thermal properties at room temperature. The values for diamond are taken from Ref. 22 and the values for gold, iridium and tungsten are taken from the material library in COMSOL.

Material	C_p [J/kgK]	k [W/Km]	ρ [kg/m^3]	T_{melt} [K]
Diamond	502	2 052	3 515	3 820
Au	129	318	19 282	1 337
Ir	130	148	22 500	2 739
W	132	174	19 300	3 695

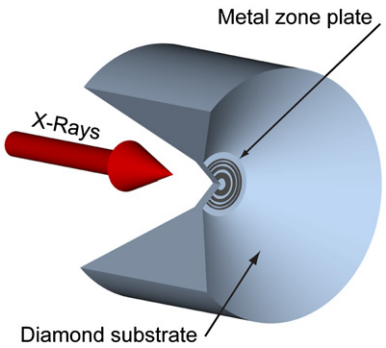

Fig. 2. Sketch of the geometry proposed for the direct beam. A metal zone plate is mounted in the center of a cone shaped diamond substrate and the edge of the substrate is cooled.

3. Theory

3.1. Transient heat transfer

The aim of this paper is to simulate the transient heat transfer that takes place after the zone plate is heated by an X-ray free electron pulse. When an X-ray photon is absorbed in a material it will transfer its energy to the electrons, for instance in form of photoelectrons and Auger electrons. This is taking place on an ultrafast time scale between femtoseconds and picoseconds. During this time the material is in a highly non-equilibrium state and no well-defined temperature exists. After some picoseconds the electrons will excite phonons and a state of local thermal equilibrium is reached. The processes taking place during and shortly after the pulse are only expected to be relevant for damage if the absorbed dose in the zone plate is close to the melting dose [21]. This has also been confirmed experimentally at the soft X-ray free electron laser facility FLASH in Hamburg [22]. For the zone plate designs discusses here the doses in the material and substrate are all well below the melting doses. Therefore, it is

enough to consider the heat transfer that takes place on longer time scales, after thermalization has occurred. In this case a macroscopic description is valid and the well-known heat equation can be used to calculate the time evolution of the temperature T:

$$\frac{dT}{dt} - \frac{k}{\rho Cp}\nabla^2 T = Q \tag{3}$$

3.2. Thermal boundary resistance

Whenever heat flows through a boundary between two different materials, it experiences a thermal boundary resistance (TBR) [23]. The result of the TBR is a discontinuity in temperature across the interface. The heat flux across the interface is given by

$$\frac{dQ}{dt} = h_{Bd}\Delta T \tag{4}$$

where dQ/dt is heat flux, ΔT is the temperature difference across the interface and h_{Bd} is the thermal conductivity of the boundary in units of W/m^2K. The resistance arises because a phonon from one material is not perfectly transmitted into the other material. Two basic models to describe the TBR are the acoustic mismatch model (AMM) [23] and the diffusive mismatch model (DMM) [23]. The AMM uses the acoustical counterpart of the Fresnel equations and the difference in acoustical impedance to calculate the probability for a phonon to cross the interface. In the case of DMM, the probability is calculated from the phonon density of states in the two materials. If the phonon spectrums are similar, the probability for a phonon to cross the interface is high and reversely if they are dissimilar, the probability is low.

The acoustical properties and phonon spectrums for metals and dielectrics are quite different and a significant TBR can be expected between the metal zone plate and the diamond

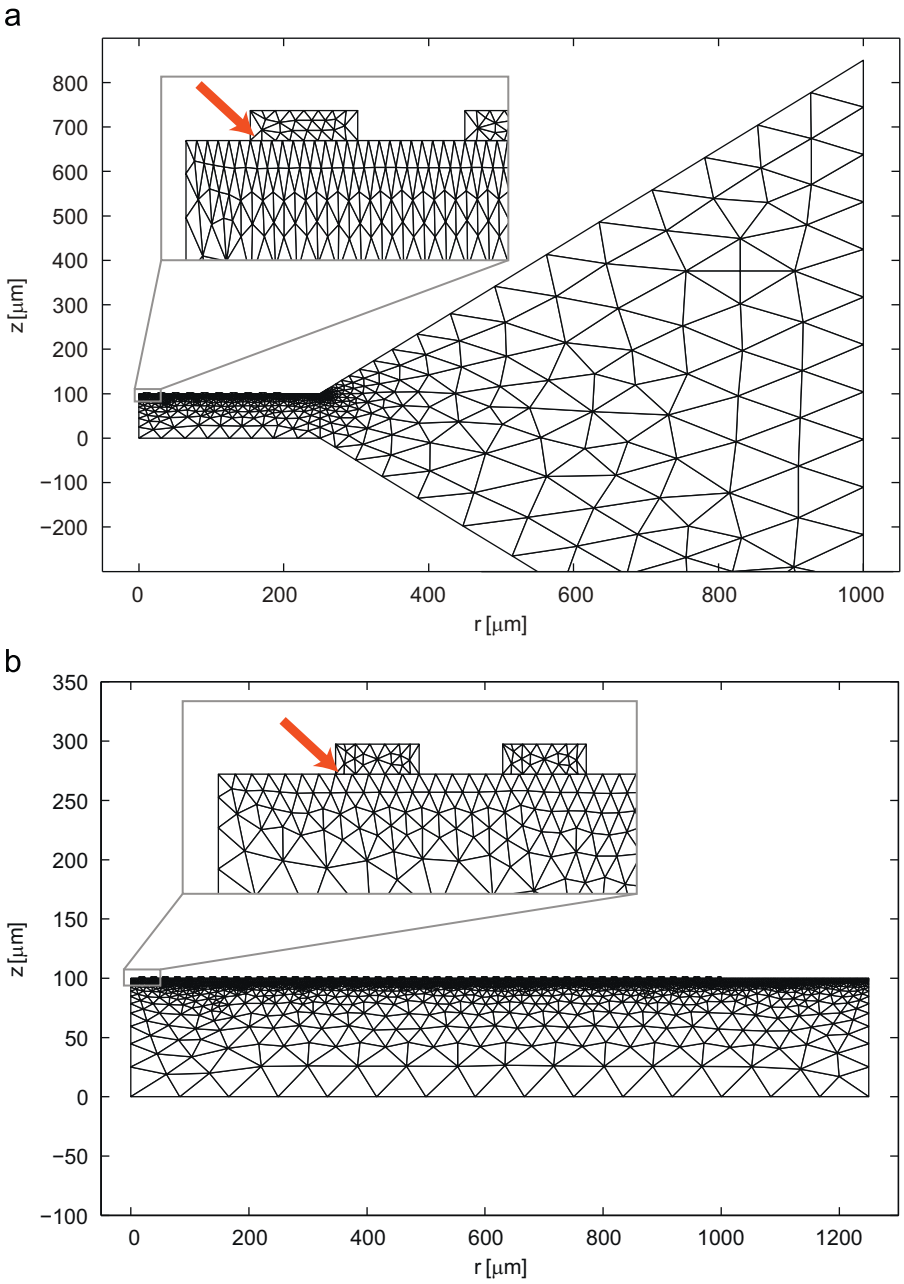

Fig. 3. The geometry and mesh for (a) the 400 μm diameter zone plate in the direct beam and (b) the 2 mm diameter zone plate behind the monochromator. The arrows indicate the hottest points in the optics and are the points for which the temperatures are presented in Section 4.

substrate. However, despite the existence of different models the exact value of the TBR is difficult to calculate since it depends on the interface quality between the two materials [23]. Measurements suggest that the conductivity is around 40 MW/m^{2}K for gold on diamond [24] and this is the value used in the simulations. Since all the investigated zone plate materials have similar acoustic properties, the simulations use the same boundary conductivity value for all materials.

3.3. Numerical implementation

To calculate the transient temperature in the zone plate and substrate, the heat equation (Eq. (3)) was solved numerically using the finite element method. The software used was COMSOL Multiphysics 3.5. The circular symmetry of the zone plate made it possible to simplify the full 3D problem to a 2D problem which results in greatly reduced computation times. Furthermore, the actual zone plate pattern was replaced by a circular grating with constant period. This was done to simplify the generation of the geometry and mesh. Since the area of obscuring zones is the same for the real pattern and the simplified one the results for the simplified pattern are also valid for the real zone plate. Fig. 3 shows the geometry and mesh used in the simulations.

Material parameters for the different metals were taken from the material library included in COMSOL. For the diamond substrate, the material parameters used originate from the compendium *CVD diamond booklet* [25], as provided by Diamond Materials GmbH, a commercial supplier of CVD diamond. All material parameters are temperature dependent and the simulations use bulk values since the error arising from size effects are expected to be comparably small. As an example, theory and measurements predict a reduction in thermal conductivity of gold to about 60% of the bulk value for structure sizes discussed here [26,27]. Although this is a significant change it will have a small impact on the general behavior of the heat transfer since the main bottlenecks are the TBR and the heat transport in the substrate.

The boundary conditions for the calculations were thermal isolation for all boundaries except for the outer edge of the substrate where the temperature is fixed to 77 K. Radiation from the boundaries was not included since its contribution to the cooling is neglectable compared to the effect of cooling through the substrate. The thermal boundary resistance was included in the simulation as an infinitesimally thin layer that can handle the discontinuity in temperature between the metal zone plate and diamond substrate. The layer had a thermal boundary conductance $h_{Bd}=40$ MW/m^{2}K.

The material warm-up during one XFEL pulse was implemented as a sudden temperature increase, which is calculated from the amount of absorbed energy as a function of r and z. Assuming a Gaussian beam, the distribution of the absorbed energy is determined by the FWHM of the beam and the absorption length l_{abs} in the material. Using the relation $\Delta Q=mC_p\Delta T$, where m is the mass, one can write the instantaneous temperature increase in one pulse ΔT_{Pulse} as

$$\Delta T_{pulse}=\int_0^{Q_0}\frac{Q}{2\pi\sigma^2 l_{abs}\rho C_p(T)}e^{-r^2/2\sigma^2}e^{-z/l_{abs}}dQ \tag{5}$$

where Q_0 is the pulse energy, $\sigma=FWHM/2.35$ and $C_P(T)$ is the temperature dependent heat capacity. The integration over Q is needed to handle the large temperature dependence of the heat capacity, especially at low temperature. The integral was solved numerically for every new pulse.

To simulate the temperature evolution after one pulse, the transient heat equation was solved using an initial temperature calculated as the sum of the ambient temperature $T_0=77$ K and the temperature increase ΔT_{Pulse}. The initial time step used was 10^{-10} s and the temperature was solved for times from $t=0$ s to $t=t_{end}$, where t_{end} is a time large enough such that the temperature everywhere has reached the ambient temperature T_0.

When simulating a full pulse train of the XFEL, the strategy was to solve the transient heat equation repeatedly between two consecutive pulses. The temperature rise in every pulse was calculated as described above. Since the heat capacity is temperature-dependent, the temperature increase will be slightly different for each new pulse.

4. Results and discussion

4.1. Single pulse

In this section we present the simulation results for the two designs suggested in Section 2 and the case when a single FEL pulse hits the optics. Fig. 4 shows the temperature evolution in the center of a 400 um diameter zone plate placed in the direct beam. This is the hottest point on the whole optic, indicated by an arrow in Fig. 3a. The initial instant temperature increase in one time step for the three different materials was calculated using Eq. (5) at an initial temperature of 77 K. The temperature curve consists of two main parts, a fast decrease followed by a slower one. The first part lasts until $t=10^{-7}$ s and is a result of heat flowing from the hot zone plate layer down into the thermal bulk of the diamond substrate. The slower process indicates the transfer of accumulated heat inside the substrate to the cooled edge of the substrate. Accordingly the time to cool down to the initial temperature will depend on the geometry and takes about 3 μs for the 400 μm zone plate. The maximum temperature directly after the FEL pulse is 314 K for gold, 305 K for iridium and 388 K for tungsten. All temperatures are well below the melting temperature of the respective materials. The observed difference is a direct result of the difference in heat capacity C_p. However, the difference in thermal conductivity k does not have a large impact on the cooling behavior since it is mainly determined by the heat transfer through the diamond substrate.

Fig. 5 shows the temperature evolution in a 2 mm diameter zone plate placed after a monochromator. The temperature increase for the different materials is only about 1/10 of the value for the direct beam. This is a direct result of the reduction in

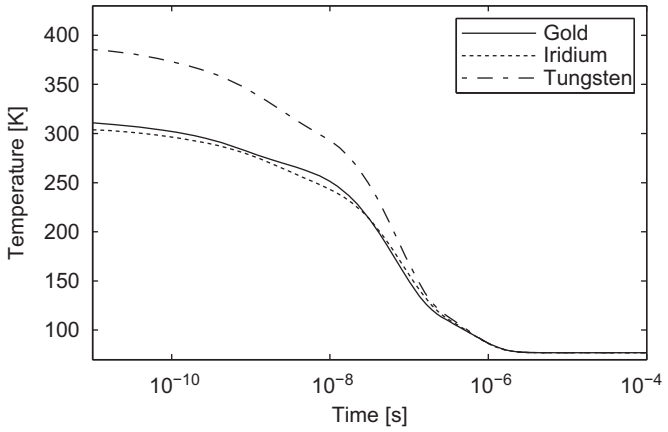

Fig. 4. Temperature evolution in a 400 μm diameter zone plate made of gold, iridium or tungsten after illumination by a single XFEL pulse of 2 mJ energy. The temperature shown is for the hottest point in the optic, indicated by an arrow in Fig. 3a.

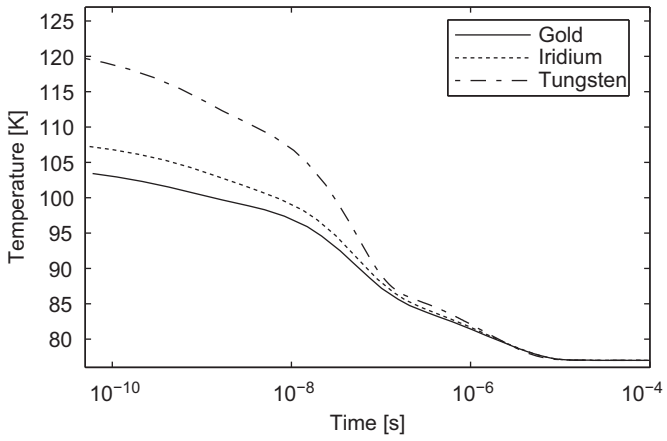

Fig. 5. Temperature evolution in a 2 mm diameter zone made of gold, iridium or tungsten after illumination by a single XFEL pulse of 0.2 mJ energy (behind monochromator). The temperature shown is for the hottest point in the optic, indicated by an arrow in Fig. 3b.

intensity by a factor of 10. The curves show the same characteristics of a fast initial part and a second slower part. The slow part is extended to about 10 μs where the initial temperature is reached. The slower cooling, as compared to the direct beam design, is a result of the increased diameter. The temperature directly after a pulse is 104 K for gold, 108 K for iridium and 121 K for tungsten. These temperatures are far below room temperature and a cooling to 77 K might not be necessary.

It is interesting to compare the time to reach 77 K with the pulse separations at the different facilities. The repetition rate of 120 Hz at LCLS corresponds to a pulse separation of 8.3 ms which is much longer than even the slower cooling time of 10 μs for the large zone plate. In other words, the zone plate will have plenty of time to reach 77 K before the next pulse arrives. The same is of course also true for the 60 Hz repetition rate at SCSS. For these two facilities, one can consider simpler cooling schemes than the one proposed in this paper. At the XFEL the pulse separation is only 200 ns and the zone plate will not have time to reach 77 K before the next pulse. In this case the full pulse train has to be simulated in detail, as discussed in the next section.

4.2. Pulse train

Here we present the simulation results for a full XFEL pulse train consisting of 3000 pulses spaced by 200 ns. Fig. 6 shows the temperature during a pulse train in a 400 μm diameter zone plate in the direct beam made of gold (a), iridium (b) and tungsten (c). The figures are divided into two parts where the left part shows the temperature for the first ten pulses and the right part shows the temperature for the last ten pulses. After about 300 pulses, the temperature behavior reaches a solution in which the temperature cycles between a maximum and a minimum value. The temperature fluctuations are 223 K for gold, 201 K for iridium and 279 K for tungsten. After the pulse train is over, the temperature decreases to 77 K as discussed in the previous section. From the simulations, one can see that the cooling provided by the diamond substrate is sufficient to keep the zone plate well below the melting temperature throughout a full pulse train. However, the large and fast temperature fluctuations might be a challenging problem.

Fig. 7 shows the temperature during a pulse train in a 2 mm diameter zone plate, made of gold (a), iridium (b) and tungsten (c), behind a monochromator. A constant average temperature is reached after about 400 pulses and the fluctuations are 24.1 K for gold, 23.5 K for iridium and 32.4 K for tungsten. The reduced intensity in combination with the effective cooling keeps the zone plates well below room temperature during the pulse train. It is clear that the average temperature will not be a problem and that the small fluctuations are manageable. Moreover, it does not seem to be crucial to use cooling down to 77 K. As an example, simulations not shown indicate that a cooling at 300 K is enough to keep the zone plate at a temperature below 600 K.

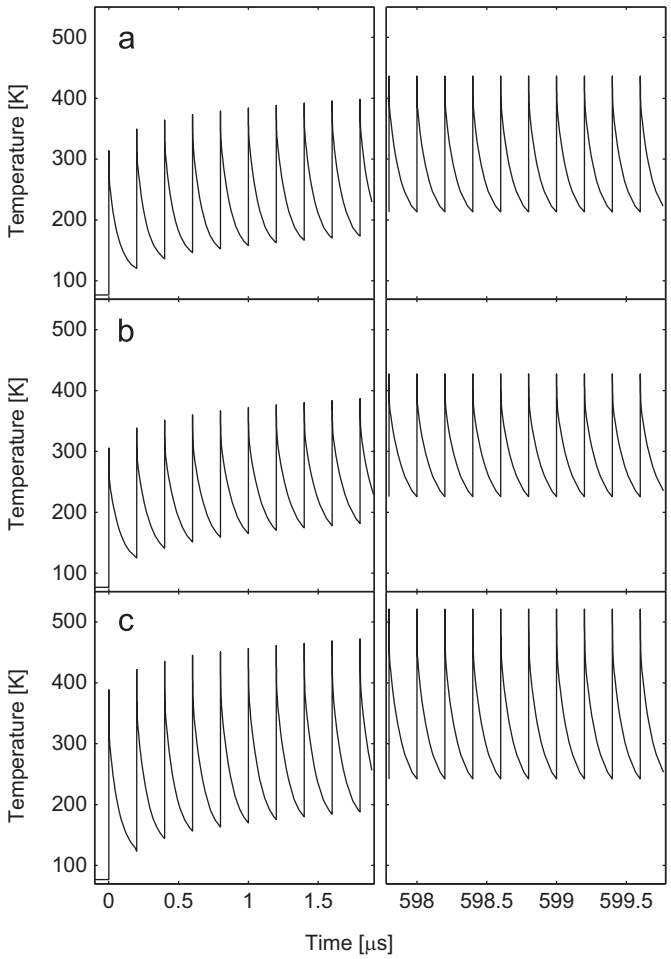

Fig. 6. Temperature in a 400 μm diameter zone plate, made of (a) gold, (b) iridium and (c) tungsten, during a full XFEL bunch train. The zone plate is placed in the direct beam and the temperature is shown for the hottest point in the optic, indicated by an arrow in Fig. 3a. The bunch train consists of 3000 pulses and the left part of the figure shows the first ten pulses and the right one shows the last ten pulses.

The thermal problems are drastically reduced when working behind the monochromator, as expected. The price one has to pay is a reduction in photon flux. However, the larger area of the zone plate partially compensates for the lower intensity. For the parameters described in this paper, the intensity in the focus when using a monochromator is 86% of that achieved by the smaller zone plate in the direct beam. The two zone plates provide equal intensity if the beam size is increased to 1085 μm and for all beam sizes above this value, the zone plate behind the monochromator provides the largest flux in a diffraction-limited focus.

5. Conclusions

In this paper the possibility for metal zone plates to survive the high heat load of an X-ray free electron laser was investigated.

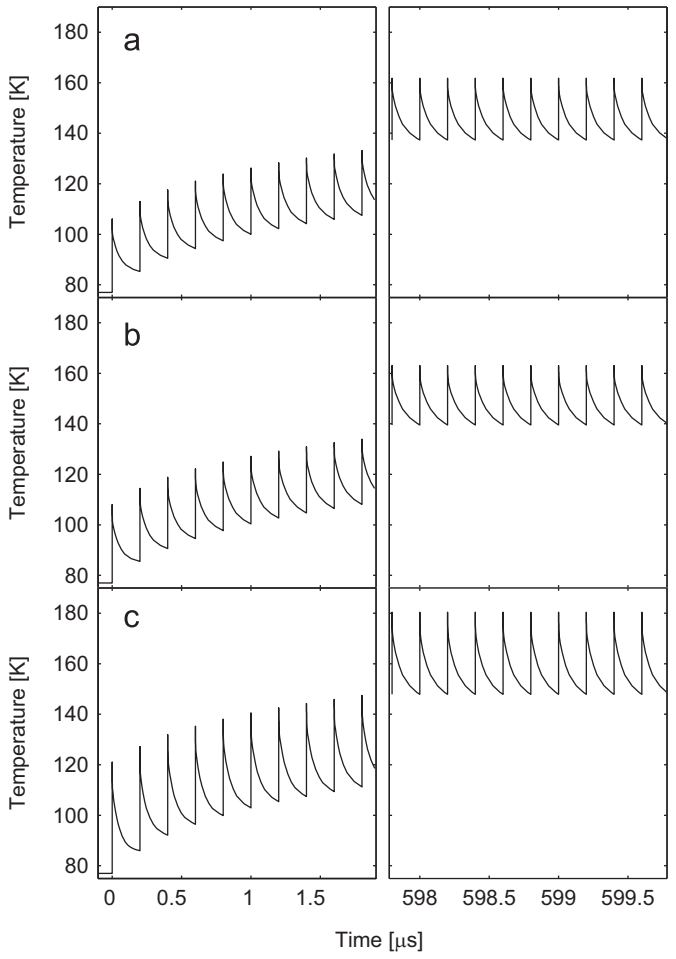

Fig. 7. Temperature in a 2 mm diameter zone plate, made of (a) gold, (b) iridium and (c) tungsten, during a full XFEL bunch train. The zone plate is placed behind a monochromator and the temperature is shown for the hottest point in the optic, indicated by an arrow in Fig. 3b. The bunch train consists of 3000 pulses and the left part of the figure shows the first ten pulses and the right one shows the last ten pulses.

The design proposed consists of a metal zone plate on a diamond substrate, cooled to 77 K. The bandwidth of the direct beam limits the number of zones to 1000, which corresponds to a diameter of 400 μm for a 100 nm outermost-zone-width zone plate. An alternative is the use of a larger 2 mm zone plate placed behind a monochromator. The simulation results for the direct beam show that the zone plate is heated several hundred Kelvin in a single pulse. However, the temperature increase is well below the melting temperature and the zone plate should not melt after a single pulse. During a pulse train, the zone plate is heated to a temperature between 200 and 600 K. This is again well below the melting temperature but the influence of the rapid and large temperature fluctuations has to be investigated further. For the case of a larger zone plate behind a monochromator the temperature increase in a single pulse and during a pulse train is small. The fluctuations are in the range of 20–30 K and should be manageable.

The thermal simulations in this paper alone cannot answer the question if metal zone plates will survive in a hard X-ray FEL beam. The simulations suggest that the zone plates should not melt but is possible that other effects such as stress or strain in the optic due to thermal expansion will prove fatal. It should also be pointed out that the exact value of the TBR between the metal zone plate layer and the diamond substrate is not known exactly and has a certain influence on the outcome of the calculations. Nevertheless, the presented results already give valuable indications on the temperature range to be expected and can be used as a basis for future heat test investigations of fabricated nanostructures.

References

[1] LCLS Conceptual design report, Stanford 2002.
[2] European XFEL Technical design report, Hamburg 2007.
[3] SCSS Conceptual design report, Japan 2006.
[4] H. Mimura, S. Matsuyama, H. Yumoto, H. Hara, K. Yamamura, Y. Sano, M. Shibahara, K. End, Y. Mori, Y. Nishino, K. Tamasaku, M. Yabashi, T. Ishikawa, K. Yamauchi, Jpn. J. Appl. Phys. Part 2-Lett. Express Lett. 44 (2005) L539.
[5] C.G. Schroer, B. Benner, M. Kuhlmann, O. Kurapova, B. Lengeler, F. Zontone, A. Snigirev, I. Snigireva, H. Schulte-Schrepping, in: S.G. Biedron, W. Eberhardt, T. Ishikawa, R.O. Tatchyn (Eds.), SPIE, Denver, CO, USA, 2004, pp. 116–124.
[6] J. Vila-Comamala, K. Jefimovs, J. Raabe, T. Pilvi, R.H. Fink, M. Senoner, A. Maassdorf, M. Ritala, C. David, Ultramicroscopy 109 (2009) 1360.
[7] W. Chao, J. Kim, S. Rekawa, P. Fischer, E.H. Anderson, Opt. Express 17 (2009) 17669.
[8] J. Reinspach, M. Lindblom, O. von Hofsten, M. Bertilson, Hans M. Hertz, A. Holmberg, AVS (2009) 2593.
[9] H.N. Chapman, A. Barty, M.J. Bogan, S. Boutet, M. Frank, S.P. Hau-Riege, S. Marchesini, B.W. Woods, S. Bajt, H. Benner, R.A. London, E. Plonjes, M. Kuhlmann, R. Treusch, S. Dusterer, T. Tschentscher, J.R. Schneider, E. Spiller, T. Moller, C. Bostedt, M. Hoener, D.A. Shapiro, K.O. Hodgson, D. Van der Spoel, F. Burmeister, M. Bergh, C. Caleman, G. Huldt, M.M. Seibert, F.R.N.C. Maia, R.W. Lee, A. Szoke, N. Timneanu, J. Hajdu, Nat. Phys. 2 (2006) 839.
[10] T. Nisius, R. Fruke, D. Schafer, M. Wieland, T. Wilhein, in: L. Juha, S. Bajt, R. Sobierajski (Eds.), 73610Y, SPIE, Prague, Czech Republic, 2009.
[11] S. Gilbert, J.F. George, in: An Analysis of the Finite Element Method, Prentice-Hall, Englewood Cliffs, N.J, 1973.
[12] J. Kirz, J. Opt. Soc. Am. 64 (1974) 301.
[13] Y.T. Chen, T.N. Lo, Y.S. Chu, J. Yi, C.J. Liu, J.Y. Wang, C.L. Wang, C.W. Chiu, T.E. Hua, Y. Hwu, Q. Shen, G.C. Yin, K.S. Liang, H.M. Lin, J.H. Je, G. Margaritondo, Nanotechnology 19 (2008) 395302.
[14] D.T. Attwood, in: Soft X-Rays and Extreme Ultraviolet Radiation, Cambridge University Press, Cambridge, 1999.
[15] Y. Feng, M. Feser, A. Lyon, S. Rishton, X. Zeng, S. Chen, S. Sassolini, W. Yun, J. Vac. Sci. Technol. B 25 (2007) 2004.
[16] A. Ozawa, T. Tamamura, T. Ishii, H. Yoshihara, T. Kagoshima, Microelectron. Eng. 35 (1997) 525.
[17] K. Jefimovs, J. Vila-Comamala, T. Pilvi, J. Raabe, M. Ritala, C. David, Phys. Rev. Lett. 99 (2007) 264801.
[18] P. Charalambous, in: Tony Warwick, Werner Meyer-Ilse, David Attwood (Eds.), X-RAY MICROSCOPY: Proceedings of the VI International Conference, AIP, Berkeley, CA, 2000, pp. 625–630.
[19] J. Vila-Comamala, K. Jefimovs, J. Raabe, B. Kaulich, C. David, Microelectron. Eng. 85 (2008) 1241.
[20] TESLA Conceptual design report, Part V, Hamburg 2001, 248–251.
[21] R.A. London, R. Bionta, R. Tatchyn, S. Roessler, in: R. Tatchyn, K.F. Andreas, T. Matsushita (Eds.), Optics for Fourth-Generation X-Ray Sources, SPIE Press, San Diego, USA, 2001, pp. 51–62.
[22] S.P. Hau-Riege, R.A. London, R.M. Bionta, M.A. McKernan, S.L. Baker, J. Krzywinski, R. Sobierajski, R. Nietubyc, J.B. Pelka, M. Jurek, L. Juha, J. Chalupsky, J. Cihelka, V. Hajkova, A. Velyhan, J. Krasa, J. Kuba, K. Tiedtke, S. Toleikis, T. Tschentscher, H. Wabnitz, M. Bergh, C. Caleman, K. Sokolowski-Tinten, N. Stojanovic, U. Zastrau, Appl. Phys. Lett. 90 (2007) 173128.
[23] E.T. Swartz, R.O. Pohl, Rev. Mod. Phys. 61 (1989) 605.
[24] R.J. Stoner, H.J. Maris, Phys. Rev. B 48 (1993) 16373.
[25] http://www.diamond-materials.com/downloads/cvd_diamond_booklet.pdf.
[26] G. Chen, P. Hui, Appl. Phys. Lett. 74 (1999) 2942.
[27] T. Yamane, Y. Mori, Si Katayama, M. Todoki, J. Appl. Phys. 82 (1997) 1153.